

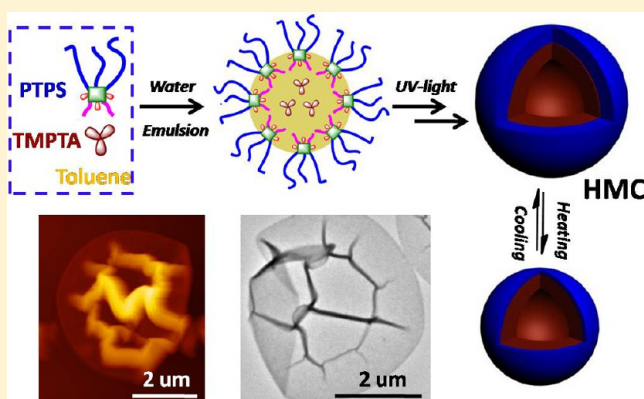
Responsive Hybrid Microcapsules by the One-Step Interfacial Thiol–Ene Photopolymerization

Dandan Liu, Bing Yu, Xuesong Jiang,* and Jie Yin

School of Chemistry and Chemical Engineering, State Key Laboratory for Metal Matrix Composite Materials, Shanghai Jiao Tong University, Shanghai 200240, People's Republic of China

Supporting Information

ABSTRACT: We here demonstrated a general, convenient, and robust method to fabricate the hybrid microcapsules through the one-step thiol–ene photopolymerization at the interface between toluene and water. In the presence of amphiphilic polyhedral oligomeric silsesquioxane (POSS) containing thiol groups (PTPS) as reactive surfactants and trimethylolpropane triacrylate (TMPTA) as a cross-linker, the wall of hybrid microcapsules can be photo-cross-linked. The obtained hybrid microcapsules (HMCs) were well-characterized by scanning electron microscopy (SEM), transmission electron microscopy (TEM), atomic force microscopy (AFM), and confocal laser scanning microscopy (CLSM). The results revealed that the obtained HMCs are uniform with the tunable size in diameter (2–4 μm) and wall thickness (55–120 nm). The size of HMCs increased with the increasing content of toluene. The wall thickness of HMCs decreased with the increasing content of cross-linker TMPTA. Furthermore, HMCs are thermoresponsive in aqueous solution, can encapsulate both hydrophobic and hydrophilic dyes, and can be used in the controlled dispersion of dyes in different mediums. It is believed that this simple, robust, and general method to fabricate the hybrid microcapsules will extend the potential application fields of microcapsules, such as in the controlled dispersion and drug delivery.



1. INTRODUCTION

Functional microcapsules with the tunable size and thickness of the wall are of both scientific and technological importance because of their potential applications in encapsulation for the controlled release of drugs, enzymes, dyes, and paints and the protection of active species.^{1–10} The wall of the microcapsules can protect the trapped species, such as drugs and dyes, and release them at a controlled speed.¹¹ Functional microcapsules can be used as microcarriers and provide ideal models for investigations of permeability and response from nano- to microscale.¹² As a result, much effort has been devoted to fabricate these functional microcapsules.^{5,13–24} To develop a robust, general, and simple method to prepare the functional microcapsules plays a critical role in their practical applications.^{25,26} Among the established techniques, self-assembly of amphiphilic block co-polymer,^{12–14,27} layer-by-layer (LBL) assembly on the sacrificial core,^{2,4,5,28} and emulsion polymerization^{15,17,25,29–31} are most widely used in the preparation of the functional microcapsules. On the basis of the self-assembly of the amphiphilic diblock co-polymer in a methanol/water solvent mixture, Du et al. prepared hybrid capsules, followed by the gelation process to fix the capsular morphology.^{13,14} Using inorganic silica particles as the sacrificial core, Caruso's group fabricated a variety of functional microcapsules through LBL

assembly, followed by the removal of the core in HF aqueous solution.^{22,32–37} These novel studies really enriched the technologies for the fabrication of functional capsules and extended their application fields. For these two methods, however, there are some limitations, such as the complex process in the preparation. In the LBL approach, for example, the sacrificial templates must be removed by the chemical etching to obtain the hollow structure, and this process is not always compatible with drugs that have to be encapsulated.⁵

Therefore, the emulsion polymerization, which does not need a sacrificial core and can minimize the number of processing steps, would be more appealing for large-scale fabrication of microcapsules. In addition, this approach is usually environmentally friendly because the medium is water. Herein, we report a general, simple, and robust approach to prepare the responsive hybrid microcapsules (HMCs) through the emulsion thiol–ene photopolymerization. Because of the significant advantages, such as the fast curing speed, insensitivity to oxygen, and easy control, thiol–ene photopolymerization is very convenient and environmentally benign and can be performed at room temperature in

Received: January 10, 2013

Revised: March 4, 2013

Published: April 2, 2013

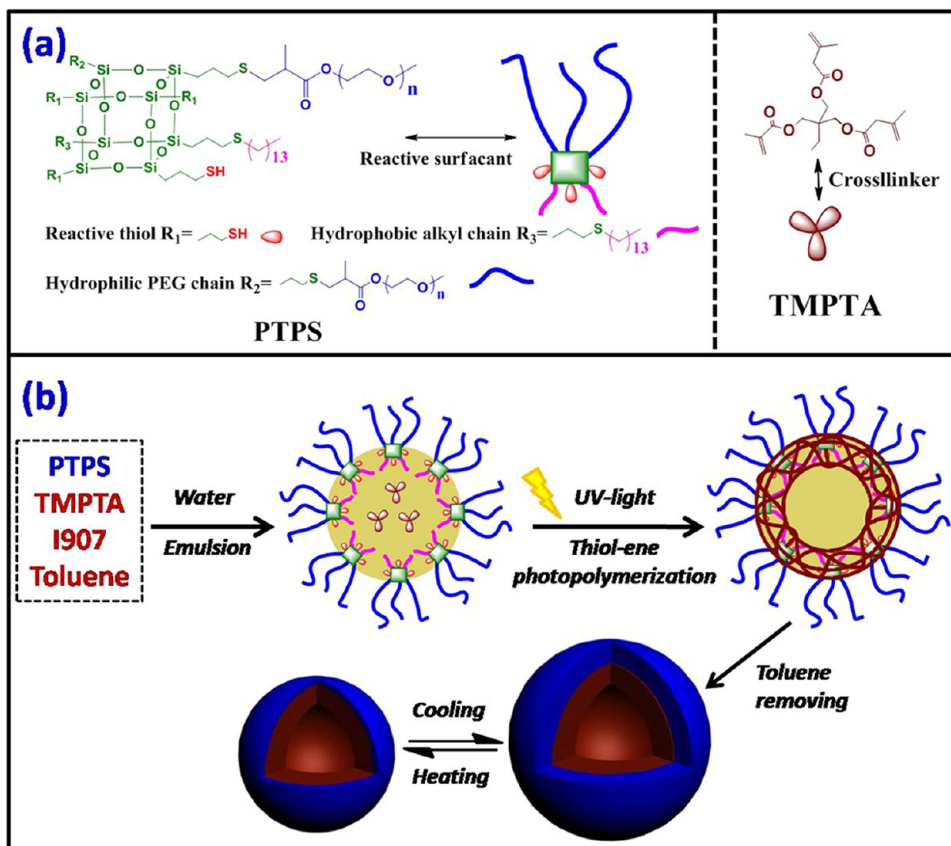


Table 1. Feed Ratio, Size in Diameter, Thickness of the Wall, and PDI of the Obtained HMCs

number	feed ratio		size		
	PTPS/TMPTA/toluene ^a	PTPS/TMPTA ^b	diameter ^c (μm)	wall thickness ^c (nm)	PDI ^d
HMC1	1:0.85:16	1:12	2.0	130	0.107
HMC2	1:0.85:32	1:12	3.0	80	0.160
HMC3	1:0.85:48	1:12	4.0	55	0.164
HMC4	1:1.70:48	1:24	3.3	100	0.186
HMC5	1:2.55:48	1:36	2.6	125	0.140
HMC6	1:2.55:96	1:36	3.0	100	0.183

^aThe feed ratio refers to the weight ratio. The total concentration of the mixture of PTPS/TMPTA/toluene in water is kept for 10 mg/mL. ^bThe feed ratio refers to the molar ratio. ^cThe diameter and wall thickness were obtained by statistical analysis from SEM images, in which 50 HMCs were counted. ^dPDI refers to the polydispersity index also obtained from SEM images.

Scheme 1. (a) Structure of Reactive Surfactant PTPS and Cross-linker TMPTA and (b) Whole Strategy To Fabricate the HMCs through Thiol–Ene Photopolymerization on the Interface between Toluene and Water



the presence of oxygen.^{38–46} HMCs are of our interest because the inorganic component as a building block for the wall of microcapsules can lead to high stability.^{19,47–52} As the smallest precisely defined cubic silica nanoparticle, polyhedral oligomeric silsesquioxane (POSS) is widely used in the preparation of the novel hybrid materials and can enhance their performance, such as mechanical strength and thermal stability.^{51–56} Meanwhile, HMCs with response to environmental stimuli, such as the temperature, can be defined as the smart materials, which can find the potential application in some fields, such as the controlled drug delivery, dispersion, and encapsulation of guest molecules.^{26,33,35,57–59}

Using thiol groups containing POSS (PTPS) as a reactive surfactant, we prepared a series of uniform-sized responsive HMCs with tunable size and wall thickness through the one-pot oil/water interfacial thiol–ene photopolymerization in this paper.

A mixture of the hydrophobic cross-linker trimethylolpropane triacrylate (TMPTA) and toluene was emulsified into a water phase to obtain an oil-in-water (O/W) emulsion using PTPS as stabilizers. Upon ultraviolet (UV) light exposure, the thiol–ene photopolymerization takes place at the interface between toluene and water phase, leading to the formation of the cross-linked shell. The resulting HMCs are responsive to the environmental temperature and can be applied in the controlled dispersion of both hydrophobic and hydrophilic dyes in water.

2. EXPERIMENTAL SECTION

2.1. Measurement. ¹H nuclear magnetic resonance (NMR) spectra was carried out on a Mercury Plus spectrometer (Varian, Inc., Palo Alto, CA), operating at 400 MHz using CDCl_3 as the solvent and tetramethylsilane (TMS) as an internal standard at room temperature.

Fourier transform infrared (FTIR) spectra measurements were carried out with a Spectrum 100 Fourier transformation infrared

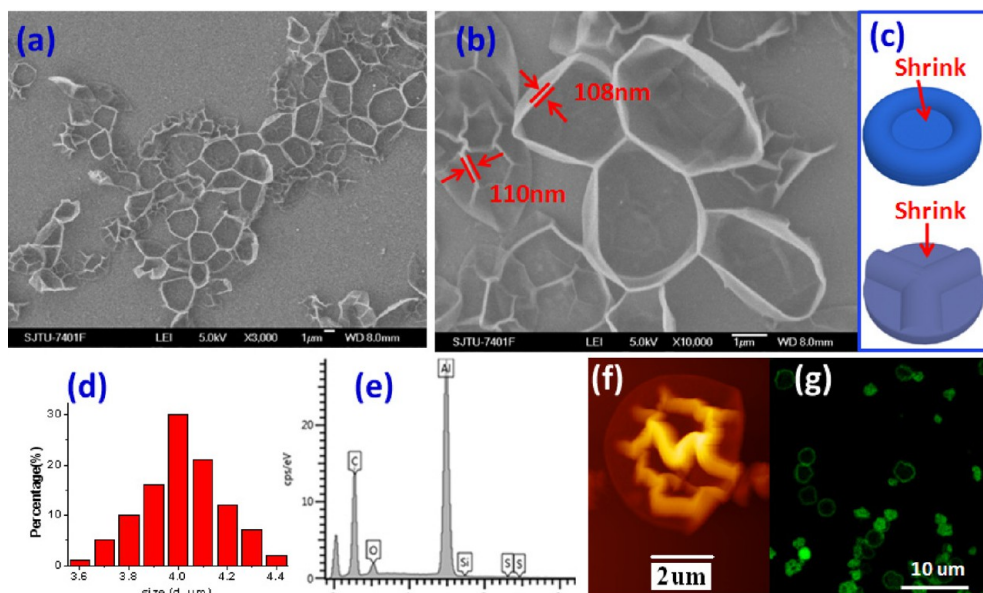


Figure 1. (a) SEM image of the hybrid microcapsule HMC3 (1:0.85:48 PTPS/TMPTA/toluene). (b) Detailed view of the SEM image. (c) Proposed sketch of the deforming of the microcapsule. (d) Size distribution histogram of HMC3 determined by SEM images. A total of 50 microcapsules were counted for the distribution. (e) EDX graph of HMC3. (f) AFM image and (g) fluorescence microscope images (CLSM) of PY-functioned HMC3.

absorption spectrometer (Perkin-Elmer, Inc., Waltham, MA). The samples were prepared by dropping the polymer solution onto a KBr film and dried below an infrared lamp.

The scanning electron microscopy (SEM) images were obtained using a JSM-7401F (JEOL, Ltd., Japan) field emission scanning electron microscope operated at an acceleration voltage of 5 kV. The samples were prepared by dropping the HMC solution onto silica wafers and air-drying the silica wafers at room temperature. Then, the samples were sputter-coated with gold before examination. With regard to EDX analysis, the samples were prepared by dropping the HMC solution onto aluminum foil, which were air-dried at room temperature.

The transmission electron microscopy (TEM) images were obtained using a JEM-2100 (JEOL, Ltd., Japan) transmission electron microscope operated at an acceleration voltage of 200 kV. The sample was prepared by dropping HMC solution onto copper grids coated with a thin carbon film, while the excess solution was removed by filter paper and air-dried at room temperature.

Atomic force microscopy (AFM) images were taken by SII Nanonavi E-sweep under ambient conditions. AFM was operated in tapping mode using silicon cantilevers with a force constant of 40 N m^{-1} . The samples were prepared by dropping the HMC solution onto a mica sheet.

The dynamic light scattering (DLS) measurements were performed in the PTPS microcapsule solution using a ZS90 Zetasizer Nano ZS instrument (Malvern Instruments, Ltd., U.K.) equipped with a multi- τ digital time correlation and a 4 mW He-Ne laser ($\lambda = 633 \text{ nm}$) at an angle of 90° . Regularized Laplace inversion (CONTIN algorithm) was applied to analyze the obtained autocorrelation functions. The concentration of HMC solution was 1 g/L.

Fluorescence images of the HMCs were viewed with confocal laser scanning microscopy (CLSM, Leica TCS-SP5, Leica, Wetzlar, Germany) equipped with UV lasers.

Thermogravimetric analysis (TGA) was carried out on TA Q5000IR thermogravimetric analyzer under nitrogen with the temperature range of $40\text{--}800^\circ\text{C}$ at a heating rate of $20^\circ\text{C min}^{-1}$.

Elemental analysis was obtained by Vario-EL IRMS (Elementar and Isoprime, Germany) elemental analyzer.

The UV-vis spectra were carried out with a UV-2550 spectrophotometer (Shimadzu, Japan).

2.2. Preparation of the HMCs. A trace amount (1 wt % of TMPTA and PTPS) of photoinitiator I907 was dissolved in a 200 mg mixture of PTPS, TMPTA, and toluene with a designed weight ratio in a 25 mL vial (see Scheme S2 of the Supporting Information). Then, 20 mL of

ultrapure water was dropped into the mixture with stirring (400 rpm). After the addition of water, the solution was stirred for 1 h, followed by ultrasonic treatment for 1 h to obtain the stable milky emulsion. The obtained emulsion was exposed under an UV light-emitting diode (LED) lamp at 365 nm (the intensity is about 8.4 mW/cm^2) for 4 h with constant stirring (400 rpm). After fully photo-cross-linking, the HMCs were obtained by centrifugation/redispersion in tetrahydrofuran (THF) 3 times. The number and feed ratio of the obtained HMCs are summarized in Table 1.

3. RESULTS AND DISCUSSION

3.1. Preparation and Characterization of HMCs. The whole strategy for the fabrication of HMCs is illustrated in Scheme 1. Toluene serves as the oil phase, while multifunctional acrylate TMPTA and PTPS are the cross-linker and surfactant, respectively. Because of the amphiphilicity, PTPS containing thiol groups is used as the reactive surfactant, which plays the critical role in the preparation of HMCs. PTPS was synthesized by grafting hydrophilic polyethylene glycol (PEG) chains and hydrophobic alkyl chains to POSS-SH via the thiol-ene photoclick reaction^{54,55} (see Scheme S1 and Figures S1 and S2 of the Supporting Information). The component of PTPS was determined by the results of $^1\text{H NMR}$ and elemental analysis. It should be noted that the obtained PTPS is not a pure compound and the ratio of thiol, alkyl chain, and PEG chain in PTPS is about 3:2:3. The residue thiol groups of PTPS are used for thiol-ene photopolymerization. As a surfactant, PTPS disperses in the interface between the water and toluene phases to lead to the stable dispersion of the emulsion droplets of toluene, while the hydrophobic cross-linker TMPTA is dissolved in the toluene phase. Upon exposure of 365 nm of UV light, the free radicals from photoinitiator I907 are trapped quickly by thiol groups to form sulfur radicals, which then initiate polymerization.³³ The thiol-ene photopolymerization takes place from the outside of the oil droplets because of the location of PTPS in the interface of oil/water. Thus, the emulsion droplets can serve as templates and guide the thiol-ene photopolymerization on their surface, resulting in the formation of the cross-linked shell. After exposure by UV light for 4 h, we checked the polymerization degree

through FTIR spectroscopy. As shown in Figure S2 of the Supporting Information, the peak at 1636 cm^{-1} assigned to the double bond of TMPTA ($\text{C}=\text{C}$) cannot be observed in FTIR spectroscopy, indicating that almost all acrylate groups participated in polymerization. The cross-linked microcapsules are then obtained after the simple removal of toluene, and the hydrophilic PEG chain as the corona of HMCs can make HMCs disperse again in water easily and stably.

The obtained HMCs were carefully characterized. As shown in Figure 1, taking a formation of 1:0.85:48 (HMC3) as an example, SEM images reveal the typical morphology of microcapsules (panels a–d of Figure 1). The average size of HMC3 is about $4.0 \pm 0.2\ \mu\text{m}$ in diameter with the low polydispersity index (PDI) of 0.164 (panels a and d of Figure 1), and the wall is around $55 \pm 3\ \text{nm}$ in thickness according to the analysis of Figure 1b. The aspect ratio between the diameter of HMC3 and the thickness of the wall is ~ 73 , indicating that HMC3 possesses a very thin wall. Two typical morphologies “bowl” and “Chinese Jiaozi” were observed in panels a and b of Figure 2, which should be ascribed

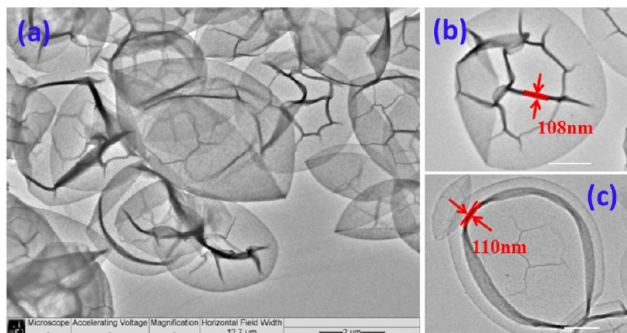


Figure 2. (a) TEM image of the hybrid microcapsule HMC3 (1:0.85:48 PTPS/TMPTA/toluene). (b) Detailed view of the TEM image morphology “Chinese Jiaozi”. The scale bars are $1\ \mu\text{m}$. (c) Detailed view of the TEM image morphology “bowl”. The scale bars are $1\ \mu\text{m}$.

to the deforming of microcapsules with a thin wall under extreme vacuum conditions.⁶⁰ Generally, the microcapsules with a thin wall tend to deform in different ways during SEM measurement, and the corresponding sketches of deforming are proposed as Figure 1c. An energy-dispersive X-ray (EDX) graph reveals the distribution of C, H, O, Si, and S elements of HMC3 (Figure 1e). The Si and S elements should be from the skeleton of POSS, suggesting that the obtained microcapsule is hybrid. The introduction of POSS into the wall of HMCs is expected to enhance the mechanical and thermal properties, which will be discussed later. Furthermore, the elemental analysis of HMC3 was conducted, and the content of the S element is 3.27%, which is close to the theoretical value of 3.25%. In other words, the content of PTPS and TMPTA in HMC3 is the same as the feed ratio, and almost all TMPTA was photo-cross-linked in the wall. AFM and CLSM images further confirmed that HMC3 keeps the typical morphology of the microcapsule (panels f and g of Figure 1). Even under the experimental conditions of AFM without vacuum, the typical deformed morphology of microcapsules was observed, which should be ascribed to the thin wall and high aspect ratio between the diameter and thickness of the wall.³⁷

As shown in Figure 2, TEM images also reveal the morphology of the uniform-sized HMC3. Panels b and c of Figure 2 present the two representative morphologies of deforming in vacuum conditions, which are in agreement with SEM results. The wall thickness of the 2-fold layer is around 110 nm, which is very close

to analysis results of SEM. The detailed view shown in TEM images reveals very smooth and homogeneous surface of HMC3, and no obvious aggregation of POSS was observed in the wall of HMC3. It should be noted that, although the thickness of the wall is thin, no microcapsules were destroyed, even under the extreme vacuum conditions in SEM and TEM measurements. This might be ascribed to the hybrid wall cross-linked highly by thiol–ene photopolymerization, which makes the obtained microcapsules robust and strong. It is well-known that the introduction of POSS into the composite materials can enhance their mechanical strength. The pure inorganic content in HMC3 is higher than 10%, and POSS still disperses homogeneously in the wall, leading to the excellent mechanical strength of the resulted HMC.^{54–56} Moreover, thiol–ene photopolymerization occurs through a step-growth reaction mechanism that offers many advantages, such as uniform structure, low polymerization shrinkage, and reduced stress. During the thiol–ene photopolymerization, trifunctional acrylate cross-linker TPMPA provides a high cross-linked network in the wall of HMC. These combining characteristics might lead to the good mechanical performance of HMC.

To verify the feasibility of our strategy, we prepared a series of HMCs through this method of interfacial thiol–ene photopolymerization. Just by changing the feed ratio of PTPS, TMPTA, and toluene simply, the uniform-sized HMCs with a tunable size in diameter and thickness of the wall can be obtained, as shown in Figure 3. The formulation, size, and thickness of the wall for the obtained HMCs are summarized in Table 1. Figure 3 provides the representative SEM images and the corresponding size distribution of the obtained HMCs. For all samples, a typical morphology of microcapsules is revealed by these SEM images. All of these HMCs did not break up, even if they adopt the extreme deformation during SEM experiments. These obtained HMCs possess the size in diameter with the range from 2.0 to $4.0\ \mu\text{m}$ and the thickness of the wall with the range from 55 to 130 nm. The PDI of all HMCs is lower than 0.2, suggesting the uniform-sized HMCs. From HMC1 to HMC3, the feed ratio of PTPS/TMPTA was fixed and the content of toluene increases. We found that the size of HMCs increases and the thickness of the wall decreases with the increasing content of toluene from HMC1 to HMC3. It is known that, in the formation of oil/water emulsion, the increasing content of the oil phase can lead to the bigger size of the emulsion droplet if the surfactant is fixed.¹⁵ The emulsion droplet determines the size of the obtained HMCs because the wall of HMC was formed by thiol–ene photopolymerization on the interface of the oil/water. Because the reactive surfactant of PTPS is fixed, the more content of toluene leads to the bigger emulsion droplet, resulting in the increasing size from HMC1 to HMC3. Therefore, the wall becomes thinner with the increasing size of HMC because the wall is made of the cross-linked network of the fixed amount of PTPS/TMPTA. When the content of PTPS and toluene are fixed, the wall thickness increases but the size of HMCs decreases with the increasing content of TMPTA from HMC3 to HMC5. It is easily understood that the thickness of the wall increases with the increasing content of the cross-linker TMPTA. The higher cross-linking density of the network of the wall, which resulted from the increasing TMPTA content, might limit the swelling of HMCs in THF or water, resulting in the reduced size during SEM measurements.

The component and thermal stability of these obtained HMCs were further investigated by TGA. Taking HMC3, HMC4, and HMC5 for example, Figure S3 of the Supporting Information

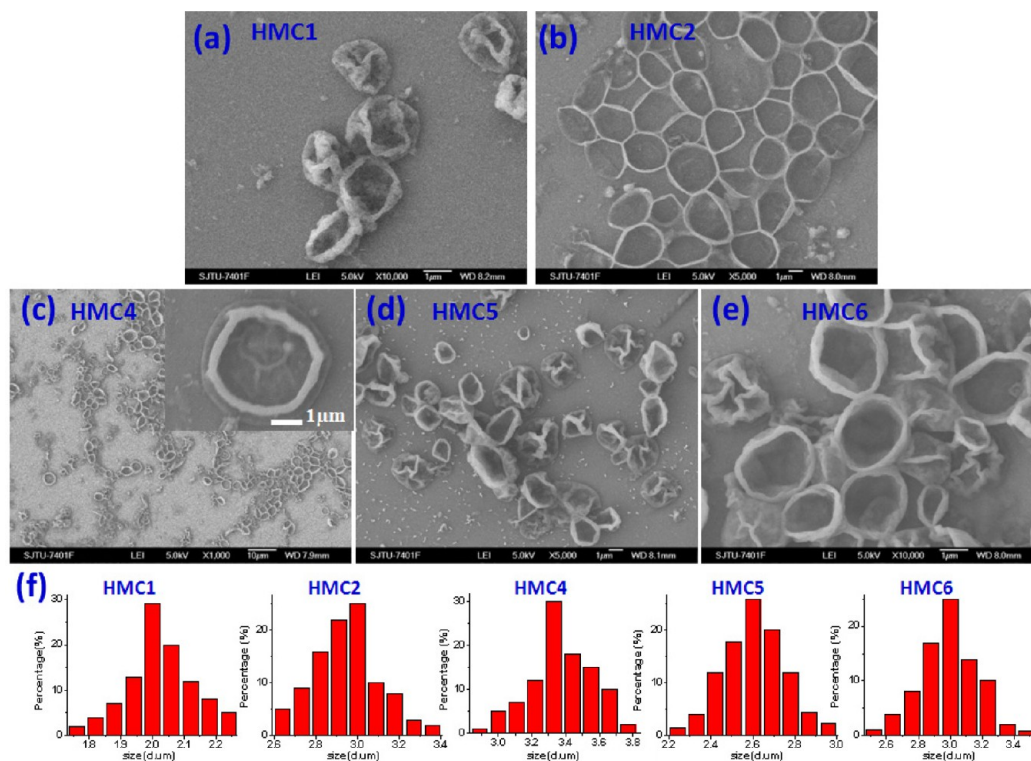


Figure 3. (a) SEM images of hybrid microcapsules HMC1, (b) HMC2, (c) HMC4, (d) HMC5, and (e) HMC6. (f) Size distribution histogram of HMCs determined by SEM images. A total of 50 microcapsules were counted for the distribution.

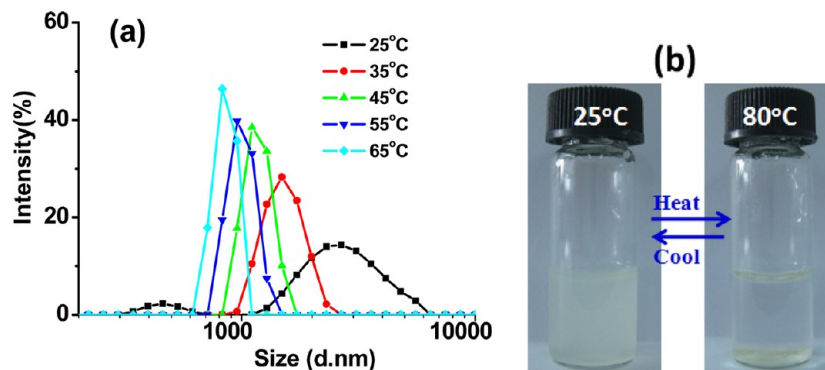


Figure 4. (a) Size distribution of HMC3 in water at different temperatures. (b) Photograph of HMC3 in water at (left) room temperature and (right) heated to a high temperature.

presents TGA curves of the obtained HMCs as well as the cross-linked TMPTA and PTPS for comparison. In comparison to PTPS, the higher decomposition temperature of HMC might be ascribed to the cross-linked structure. Because of the thermal decomposition of the PEG chain at the lower temperature, HMCs tend to decompose at a lower temperature than the cross-linked TMPTA. The weight retention of HMCs resulting from the undecomposed inorganic POSS increases with the increasing content of PTPS from HMC5 to HMC3, which is in agreement with the results of elemental analysis and the feed ratio of PTPS/TMPTA. The excellent thermal stability of HMCs might be ascribed to the presence of POSS in the cross-linking network of the wall of HMCs, which reduces the diffusion of volatiles in the hybrid material.^{57,58} In addition, the inorganic component of POSS provides additional heat capacity and stabilizes the materials against thermal decomposition.⁵⁹ Because of the nanostructural effects and flame resistance of POSS, the incorporation of POSS can improve the thermal stability of

HMCs obviously. The other factor to the excellent thermal stability of HMCs is the cross-linking network of their wall. Generally, the photo- or thermal-cured acrylate matrix exhibits the enhanced thermal performance with the increasing cross-linking density.²⁶

3.2. Responsive Behavior of HMCs and the Controlled Dispersion of Dyes. The obtained HMCs are amphiphilic because the wall of HMCs is comprised of the hydrophobic TMPTA and reactive surfactant PTPS containing PEG chains. The hydrophilic PEG chains as the corona of HMCs lead to the stable dispersion of HMCs in water. POSS was introduced into the shell of HMCs and make the shell tough rather than rigid. When heated to a high temperature, hydrogen bonds between hydrophilic polyethylene oxide (PEO) chains and water molecules are destroyed, resulting in less hydrophilicity of the wall of HMCs and, consequently, leading to the shrinkage and aggregation of HMCs in water. Therefore, the dispersion of HMCs in water is expected to be responsive to the temperature.

Taking HMC3 in water as an example, the size dependent upon the temperature is revealed by the DLS measurement (Figure 4a). The Z-average diameter of HMC3 decreases obviously with the increasing temperature from 25 to 65 °C. This phenomenon indicated that HMC3 shrinks with the increase of the temperature, which is ascribed to the temperature-responsive wall of the HMCs. When heating to the higher temperature, HMC3 dispersed stably in water at room temperature tends to aggregate and precipitate from the aqueous solution, which was clearly reflected by the change of the solution (Figure 4b).

Because of the novel characteristics of HMCs, such as facile preparation, response to the temperature, and amphiphility, HMCs can be used in the encapsulation and controlled dispersion of guest molecules. In the presence of HMC3, we investigated the dispersion behavior of dyes in different solvents. The dispersion experiments were carried out in a 5 mL vial, and the concentration of HMC3 was 1 g/L in all experiments. As a hydrophobic dye, Nile Red (NR), which is insoluble in water, was dispersed in water immediately after the addition of HMC3, which can be reflected by change of the color of the solution (Figure 5a). The dispersion of the hydrophobic NR in water

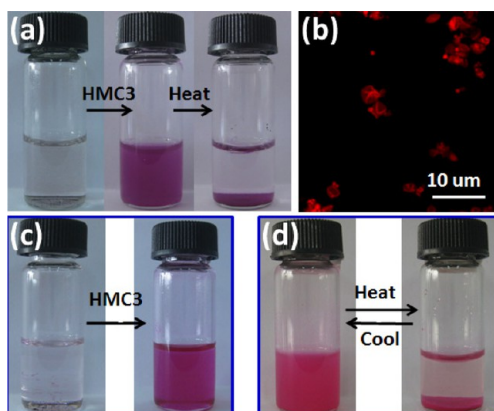


Figure 5. (a) Photographs of hydrophobic NR in water before and after the addition of HMC3 at room temperature and heated to a high temperature (80 °C). (b) Fluorescence microscope images (CLSM) of HMC3. (c). Photographs of hydrophilic RB in toluene before and after the addition of HMC3. (d) Photographs of HMC3 adsorbed RB in water at room and high temperatures (80 °C).

should be ascribed to the encapsulation of NR by HMC3, which was confirmed by the CLSM image. As shown in Figure 5b, the strong red emission of HMC3 resulted from the fluorescence of NR encapsulated in the wall of HMC3. Similarly, the hydrophilic Rose Bengal (RB) is insoluble in toluene, but RB could be dispersed in toluene in the presence of HMC3, which can also be reflected by change of the color of the solution shown in Figure 5c. UV–vis spectra of NR and RB in solution with and without HMC3 were recorded (see Figure S4 of the Supporting Information), indicating that these dyes can be easily dispersed in their poor solvents with the help of amphiphilic HMC3. In the poor solvent, the amount of NR and RB encapsulated by HMC3 was determined by UV–vis spectra. A total of 1 mg of HMC3 can encapsulate 0.59 mg of NR in water and 0.33 mg of RB in toluene. The high loading amount of dyes in HMC3 might be ascribed to its hollow structure.

Because the hybrid microcapsule of HMC3 is thermoresponsive in water, the dispersion of NR in the presence of HMC3 in water could be controlled by the temperature. A total of 2 mg of hydrophobic NR was suspended in 3 mL of water, and then 3

mg of dry HMCs was added. As shown in Figure 5a, after stirring for 20 min and ultrasonic treatment for 20 min, NR can be encapsulated in HMC3 and dispersed in water. When heated to the high temperature (80 °C), NR would precipitate with HMC3 at the bottom. This process is reversible, and NR could be dispersed in water again when shaken slightly at room temperature. It is interesting that the dispersion of the water-soluble RB in water could also be controlled by the temperature in the presence of HMC3. RB precipitated with HMC3 in water at the bottom after heating to the high temperature (Figure 5d). This indicated that the hydrophilic RB can be encapsulated by HMC3 even in water. RB can be adsorbed by the hybrid amphiphilic materials in aqueous solution,⁶⁰ which might explain why the dispersion of RB can be controlled by HMC3 in water.

4. CONCLUSION

In summary, using amphiphilic POSS containing thiol groups as the reactive surfactant (PTPS), we developed a general, convenient, and robust approach to fabricate the HMCs through the thiol–ene photopolymerization at the interface between toluene and water. The obtained HMCs were uniform with the tunable size in diameter and wall thickness, which can be controlled by the feed ratio of PTPS, cross-linker TMPTA, and toluene. Because of the introduction of inorganic POSS in the wall, HMCs exhibited good thermal and mechanical performance. Furthermore, HMCs are thermoresponsive in aqueous solution and can be used in the controlled dispersion of dyes in different mediums. Because of the novel characteristics, such as easy preparation and temperature responsiveness, HMCs are believed to have great potential application, such as in the controlled dispersion and drug delivery.

■ ASSOCIATED CONTENT

Supporting Information

Experimental details, Scheme S1, and Figures S1–S4. This material is available free of charge via the Internet at <http://pubs.acs.org>.

■ AUTHOR INFORMATION

Corresponding Author

*Telephone: +86-21-54743268. Fax: +86-21-54747445. E-mail: ponygle@sjtu.edu.cn.

Notes

The authors declare no competing financial interest.

■ ACKNOWLEDGMENTS

We thank the National Natural Science Foundation of China (21174085 and 21274088), the Science and Technology and Education Commission of Shanghai Municipal Government (11QA1403100 and 12ZZ020), and the Shanghai Leading Academic Discipline Project (B202) for their financial support. Xuesong Jiang is supported by the SMC Project of Shanghai Jiao Tong University.

■ REFERENCES

- (1) Wu, T.; Ge, Z.; Liu, S. Fabrication of thermoresponsive cross-linked poly(*N*-isopropylacrylamide) nanocapsules and silver nanoparticle-embedded hybrid capsules with controlled shell thickness. *Chem. Mater.* **2011**, *23* (9), 2370–2380.
- (2) Gokmen, M. T.; De Geest, B. G.; Hennink, W. E.; Du Prez, F. E. “Giant” hollow multilayer capsules by microfluidic templating. *ACS Appl. Mater. Interfaces* **2009**, *1* (6), 1196–1202.

- (3) Yamamoto, T.; Dobashi, T.; Kimura, M.; Chang, C. P. An approach to analysis of pigment release from microcapsules with size distribution. *Colloids Surf., B* **2002**, *25* (4), 305–311.
- (4) Shi, J.; Zhang, L.; Jiang, Z. Facile construction of multicompartiment multienzyme system through layer-by-layer self-assembly and biomimetic mineralization. *ACS Appl. Mater. Interfaces* **2011**, *3* (3), 881–889.
- (5) Wang, X.; Jiang, Z.; Shi, J.; Liang, Y.; Zhang, C.; Wu, H. Metal–organic coordination-enabled layer-by-layer self-assembly to prepare hybrid microcapsules for efficient enzyme immobilization. *ACS Appl. Mater. Interfaces* **2012**, *4* (7), 3476–3483.
- (6) Fakhrollin, R. F.; Minullina, R. T. Hybrid cellular–inorganic core–shell microparticles: Encapsulation of individual living cells in calcium carbonate microshells. *Langmuir* **2009**, *25* (12), 6617–6621.
- (7) Wang, Y.; Bansal, V.; Zelikin, A. N.; Caruso, F. Templated synthesis of single-component polymer capsules and their application in drug delivery. *Nano Lett.* **2008**, *8* (6), 1741–1745.
- (8) Mertz, D.; Wu, H.; Wong, J. S.; Cui, J.; Tan, P.; Alles, R.; Caruso, F. Ultrathin, bioresponsive and drug-functionalized protein capsules. *J. Mater. Chem.* **2012**, *22* (40), 21434–21442.
- (9) Huang, Y.-F.; Chiang, W.-H.; Tsai, P.-L.; Chern, C.-S.; Chiu, H.-C. Novel hybrid vesicles co-assembled from a cationic lipid and PAAc-g-mPEG with pH-triggered transmembrane channels for controlled drug release. *Chem. Commun.* **2011**, *47* (39), 10978–10980.
- (10) Thombre, A. G.; Cardinal, J. R.; DeNoto, A. R.; Herbig, S. M.; Smith, K. L. Asymmetric membrane capsules for osmotic drug delivery: I. Development of a manufacturing process. *J. Controlled Release* **1999**, *57* (1), 55–64.
- (11) Lv, H.; Lin, Q.; Zhang, K.; Yu, K.; Yao, T.; Zhang, X.; Zhang, J.; Yang, B. Facile fabrication of monodisperse polymer hollow spheres. *Langmuir* **2008**, *24* (23), 13736–13741.
- (12) Dong, R.; Zhu, B.; Zhou, Y.; Yan, D.; Zhu, X. “Breathing” vesicles with jellyfish-like on–off switchable fluorescence behavior. *Angew. Chem., Int. Ed.* **2012**, *51* (46), 11633–11637.
- (13) Du, J.; Chen, Y. Preparation of organic/inorganic hybrid hollow particles based on gelation of polymer vesicles. *Macromolecules* **2004**, *37* (15), 5710–5716.
- (14) Du, J.; Chen, Y. Organic–inorganic hybrid nanoparticles with a complex hollow structure. *Angew. Chem., Int. Ed.* **2004**, *43* (38), 5084–5087.
- (15) Chen, Y.; Liang, F.; Yang, H.; Zhang, C.; Wang, Q.; Qu, X.; Li, J.; Cai, Y.; Qiu, D.; Yang, Z. Janus nanosheets of polymer–inorganic layered composites. *Macromolecules* **2012**, *45* (3), 1460–1467.
- (16) Ley, S. V.; Ramarao, C.; Gordon, R. S.; Holmes, A. B.; Morrison, A. J.; McConvey, I. F.; Shirley, I. M.; Smith, S. C.; Smith, M. D. Polyurea-encapsulated palladium(II) acetate: A robust and recyclable catalyst for use in conventional and supercritical media. *Chem. Commun.* **2002**, *10*, 1134–1135.
- (17) Chu, L.-Y.; Park, S.-H.; Yamaguchi, T.; Nakao, S.-i. Preparation of micron-sized monodispersed thermoresponsive core–shell microcapsules. *Langmuir* **2002**, *18* (5), 1856–1864.
- (18) Johnston, A. P. R.; Such, G. K.; Caruso, F. Triggering release of encapsulated cargo. *Angew. Chem., Int. Ed.* **2010**, *49* (15), 2664–2666.
- (19) Caruso, F.; Caruso, R. A.; Möhwald, H. Nanoengineering of inorganic and hybrid hollow spheres by colloidal templating. *Science* **1998**, *282* (5391), 1111–1114.
- (20) Wei, Z.; Wang, C.; Zou, S.; Liu, H.; Tong, Z. Chitosan nanoparticles as particular emulsifier for preparation of novel pH-responsive Pickering emulsions and PLGA microcapsules. *Polymer* **2012**, *53* (6), 1229–1235.
- (21) Li, J.; Wang, Y.; Zhang, C.; Liang, F.; Qu, X.; Li, J.; Wang, Q.; Qiu, D.; Yang, Z. Janus polymeric cages. *Polymer* **2012**, *53* (17), 3712–3718.
- (22) Leung, M. K. M.; Such, G. K.; Johnston, A. P. R.; Biswas, D. P.; Zhu, Z.; Yan, Y.; Lutz, J.-F.; Caruso, F. Assembly and degradation of low-fouling click-functionalized poly(ethylene glycol)-based multilayer films and capsules. *Small* **2011**, *7* (8), 1075–1085.
- (23) Zhang, L.; Wu, J.; Wang, Y.; Long, Y.; Zhao, N.; Xu, J. Combination of bioinspiration: A general route to superhydrophobic particles. *J. Am. Chem. Soc.* **2012**, *134* (24), 9879–9881.
- (24) Bachtis, A. R.; Kiparissides, C. Synthesis and release studies of oil-containing poly(vinyl alcohol) microcapsules prepared by coacervation. *J. Controlled Release* **1996**, *38* (1), 49–58.
- (25) Chen, T.; Du, B.; Fan, Z. Facile fabrication of polymer nanocapsules with cross-linked organic–inorganic hybrid walls. *Langmuir* **2012**, *28* (30), 11225–11231.
- (26) Liang, X.; Kozlovskaya, V.; Chen, Y.; Zavgorodnya, O.; Kharlampieva, E. Thermosensitive multilayer hydrogels of poly(*N*-vinylcaprolactam) as nanothin films and shaped capsules. *Chem. Mater.* **2012**, *24* (19), 3707–3719.
- (27) Wang, Z.; van Oers, M. C. M.; Rutjes, F. P. J. T.; van Hest, J. C. M. Polymersome colloidosomes for enzyme catalysis in a biphasic system. *Angew. Chem. Int. Ed.* **2012**, *51* (43), 10746–10750.
- (28) Kharlampieva, E.; Kozlovskaya, V.; Sukhishvili, S. A. Layer-by-layer hydrogen-bonded polymer films: From fundamentals to applications. *Adv. Mater.* **2009**, *21* (30), 3053–3065.
- (29) Utama, R. H.; Guo, Y.; Zetterlund, P. B.; Stenzel, M. H. Synthesis of hollow polymeric nanoparticles for protein delivery via inverse miniemulsion periphery RAFT polymerization. *Chem. Commun.* **2012**, *48* (90), 11103–11105.
- (30) Breitenkamp, K.; Emrick, T. Novel polymer capsules from amphiphilic graft copolymers and cross-metathesis. *J. Am. Chem. Soc.* **2003**, *125* (40), 12070–12071.
- (31) Thompson, K. L.; Chambon, P.; Verber, R.; Armes, S. P. Can polymersomes form colloidosomes? *J. Am. Chem. Soc.* **2012**, *134* (30), 12450–12453.
- (32) Ochs, C. J.; Such, G. K.; Stadler, B.; Caruso, F. Low-fouling, biofunctionalized, and biodegradable click capsules. *Biomacromolecules* **2008**, *9* (12), 3389–3396.
- (33) Such, G. K.; Tjijto, E.; Postma, A.; Johnston, A. P. R.; Caruso, F. Ultrathin, responsive polymer click capsules. *Nano Lett.* **2007**, *7* (6), 1706–1710.
- (34) Kinnane, C. R.; Such, G. K.; Caruso, F. Tuning the properties of layer-by-layer assembled poly(acrylic acid) click films and capsules. *Macromolecules* **2011**, *44* (5), 1194–1202.
- (35) Liang, K.; Such, G. K.; Zhu, Z.; Yan, Y.; Lomas, H.; Caruso, F. Charge-shifting click capsules with dual-responsive cargo release mechanisms. *Adv. Mater.* **2011**, *23* (36), H273–H277.
- (36) Postma, A.; Yan, Y.; Wang, Y.; Zelikin, A. N.; Tjijto, E.; Caruso, F. Self-polymerization of dopamine as a versatile and robust technique to prepare polymer capsules. *Chem. Mater.* **2009**, *21* (14), 3042–3044.
- (37) Ochs, C. J.; Hong, T.; Such, G. K.; Cui, J.; Postma, A.; Caruso, F. Dopamine-mediated continuous assembly of biodegradable capsules. *Chem. Mater.* **2011**, *23* (13), 3141–3143.
- (38) Kolb, H. C.; Finn, M. G.; Sharpless, K. B. Click chemistry: Diverse chemical function from a few good reactions. *Angew. Chem., Int. Ed.* **2001**, *40* (11), 2004–2021.
- (39) Hoyle, C. E.; Bowman, C. N. Thiol–ene click chemistry. *Angew. Chem., Int. Ed.* **2010**, *49* (9), 1540–1573.
- (40) McCall, J. D.; Anseth, K. S. Thiol–ene photopolymerizations provide a facile method to encapsulate proteins and maintain their bioactivity. *Biomacromolecules* **2012**, *13* (8), 2410–2417.
- (41) Killops, K. L.; Campos, L. M.; Hawker, C. J. Robust, efficient, and orthogonal synthesis of dendrimers via thiol–ene “click” chemistry. *J. Am. Chem. Soc.* **2008**, *130* (15), 5062–5064.
- (42) Hensarling, R. M.; Doughty, V. A.; Chan, J. W.; Patton, D. L. “Clicking” polymer brushes with thiol–yne chemistry: Indoors and out. *J. Am. Chem. Soc.* **2009**, *131* (41), 14673–14675.
- (43) Lee, T. Y.; Roper, T. M.; Jonsson, E. S.; Guymon, C. A.; Hoyle, C. E. Thiol–ene photopolymerization kinetics of vinyl acrylate/multifunctional thiol mixtures. *Macromolecules* **2004**, *37* (10), 3606–3613.
- (44) Hagberg, E. C.; Malkoch, M.; Ling, Y.; Hawker, C. J.; Carter, K. R. Effects of modulus and surface chemistry of thiol–ene photopolymers in nanoimprinting. *Nano Lett.* **2007**, *7* (2), 233–237.
- (45) Khire, V. S.; Lee, T. Y.; Bowman, C. N. Synthesis, characterization and cleavage of surface-bound linear polymers formed using thiol–ene photopolymerizations. *Macromolecules* **2008**, *41* (20), 7440–7447.
- (46) Zou, J.; Hew, C. C.; Themistou, E.; Li, Y.; Chen, C.-K.; Alexandridis, P.; Cheng, C. Clicking well-defined biodegradable

nanoparticles and nanocapsules by UV-induced thiol–ene cross-linking in transparent miniemulsions. *Adv. Mater.* **2011**, *23* (37), 4274–4277.

(47) Liu, G.; Zhang, H.; Yang, X.; Wang, Y. Facile synthesis of silica/polymer hybrid microspheres and hollow polymer microspheres. *Polymer* **2007**, *48* (20), 5896–5904.

(48) Fielding, L. A.; Armes, S. P. Preparation of Pickering emulsions and colloidosomes using either a glycerol-functionalised silica sol or core–shell polymer/silica nanocomposite particles. *J. Mater. Chem.* **2012**, *22* (22), 11235–11244.

(49) Lee, W.; Ni, S.; Deng, J.; Kim, B.-S.; Satija, S. K.; Mather, P. T.; Esker, A. R. Telechelic poly(ethylene glycol)–POSS amphiphiles at the air/water interface. *Macromolecules* **2007**, *40* (3), 682–688.

(50) Zhang, W.; Yuan, J.; Weiss, S.; Ye, X.; Li, C.; Muller, A. H. E. Telechelic hybrid poly(acrylic acid)s containing polyhedral oligomeric silsesquioxane (POSS) and their self-assembly in water. *Macromolecules* **2011**, *44* (17), 6891–6898.

(51) Monticelli, O.; Fina, A.; Ullah, A.; Waghmare, P. Preparation, characterization, and properties of novel PSMA–POSS systems by reactive blending. *Macromolecules* **2009**, *42* (17), 6614–6623.

(52) Strachota, A.; Kroutilová, I.; Kovářová, J.; Matějka, L. Epoxy networks reinforced with polyhedral oligomeric silsesquioxanes (POSS). Thermomechanical properties. *Macromolecules* **2004**, *37* (25), 9457–9464.

(53) Chinnam, P. R.; Wunder, S. L. Polyoctahedral silsesquioxane–nanoparticle electrolytes for lithium batteries: POSS–lithium salts and POSS–PEGs. *Chem. Mater.* **2011**, *23* (23), 5111–5121.

(54) Li, G. Polyhedral oligomeric silsesquioxane (POSS) polymers and copolymers: A review. *J. Inorg. Organomet.* **2002**, *11* (3), 123.

(55) Lichtenhan, J. D.; Otonari, Y. A.; Carr, M. J. Linear hybrid polymer building blocks: Methacrylate-functionalized polyhedral oligomeric silsesquioxane monomers and polymers. *Macromolecules* **1995**, *28* (24), 8435–8437.

(56) Phillips, S. H.; Haddad, T. S.; Tomczak, S. J. Developments in nanoscience: polyhedral oligomeric silsesquioxane (POSS)-polymers. *Curr. Opin. Solid State Mater. Sci.* **2004**, *8* (1), 21–29.

(57) Peng, B.; Liu, Y.; Shi, Y.; Li, Z.; Chen, Y. Thermo-responsive organic–inorganic hybrid vesicles with tunable membrane permeability. *Soft Matter* **2012**, *8* (48), 12002–12008.

(58) Peyratout, C. S.; Dähne, L. Tailor-made polyelectrolyte microcapsules: From multilayers to smart containers. *Angew. Chem., Int. Ed.* **2004**, *43* (29), 3762–3783.

(59) Lendlein, A.; Shastri, V. P. Stimuli-sensitive polymers. *Adv. Mater.* **2010**, *22* (31), 3344–3347.

(60) Yu, B.; Jiang, X.; Qin, N.; Yin, J. Thiol–ene photocrosslinked hybrid vesicles from co-assembly of POSS and poly(ether amine) (PEA). *Chem. Commun.* **2011**, *47* (44), 12110–12112.